

# Comparative in Vitro Analysis of Milled vs. 3D-Printed Zirconia for Emergency Dental Splints: The Effect of Printing Angle on Optical Properties

Elham Moghadas<sup>1, 2</sup>, Nazila Najari<sup>3</sup>, Elahe Tahmassebi<sup>1\*</sup>

<sup>1</sup> Research Center for Prevention of Oral and Dental Diseases, Baqiyatallah University of Medical Sciences, Tehran, Iran

<sup>2</sup> Department of prosthodontics, School of dentistry, Baqiyatallah University of medical sciences, Tehran, Iran

<sup>3</sup> Specialist in Prosthodontics, Private office

\***Corresponding Author:** Elahe Tahmassebi, Research Center for Prevention of Oral and Dental Diseases, Baqiyatallah University of Medical Sciences, Tehran, Iran, E-mail: elahe.tahmassebi.delfan@gmail.com

Received 2026-01-09; Accepted 2026-04-25; Online Published 2026-04-29

## Abstract

**Introduction:** To evaluate the optical properties of zirconia fabricated via milling and 3D printing for urgent dental restoration in trauma and reconstructive care, focusing on the impact of printing orientation—a critical parameter for point-of-care, patient-specific manufacturing.

**Method:** In this in vitro study, eighty zirconia specimens were fabricated using four methods relevant to digital workflows: conventional milling (control) and digital light processing (DLP) 3D printing at 0°, 45°, and 90° build orientations (n = 20 per group). Key aesthetic parameters—translucency parameter (TP) and surface gloss—were measured using a spectrophotometer and glossmeter, respectively, both before and after simulated clinical aging (10,000 thermocycles).

**Result:** Translucency was not significantly affected by fabrication method or aging ( $p > 0.05$ ). In contrast, surface gloss was significantly reduced by thermocycling in all groups ( $p < 0.001$ ) and was dependent on the manufacturing technique ( $p = 0.019$ ). Milled zirconia demonstrated the highest gloss. Among 3D-printed specimens, the 0° orientation yielded significantly higher gloss than the 45° or 90° orientations.

**Conclusion :** For aesthetic dental restoration in trauma care, 3D-printed zirconia can match the translucency stability of milled standards. However, its surface gloss is inferior and highly sensitive to printing angle. To integrate efficient, patient-specific 3D printing into emergency digital workflows, protocols must be optimized—favoring lower print angles (e.g., 0°)—to minimize post-processing and expedite the delivery of definitive, aesthetically satisfactory restorations.

**Keywords:** 3D Printing, Gloss, Milling, Optical Properties, Printing Angle, Translucency, Zirconia

## Introduction

Rapid, reliable, and aesthetically acceptable dental restoration is a critical component in the multidisciplinary management of craniomaxillofacial (CMF) trauma. Following acute injury, the goals shift from emergency stabilization to definitive functional and aesthetic reconstruction, often requiring precise dental prosthetics<sup>1</sup>. In this context, zirconia has emerged as a material of significant interest due to its favorable biocompatibility, high mechanical strength necessary for withstanding occlusal loads, and its potential to

achieve tooth-like aesthetics—a key factor in the psychosocial recovery of trauma patients<sup>2</sup>.

The integration of computer-aided design and computer-aided manufacturing (CAD/CAM) has been transformative, enhancing precision and reproducibility while expanding the range of processable materials<sup>3, 4</sup>. Currently, zirconia restorations are primarily fabricated via subtractive manufacturing (SM), typically the milling of pre-sintered blocks. However, this established technique presents inherent drawbacks,

including significant material waste, tool wear, geometric limitations, and the potential introduction of surface flaws that may compromise long-term performance<sup>5-7</sup>.

Additive manufacturing (AM), or 3D printing, has emerged as a promising alternative, constructing objects layer-by-layer from digital models. This paradigm offers distinct advantages for dental applications, such as reduced material consumption, greater design freedom for complex geometries, and the potential for streamlined fabrication<sup>8</sup>. Consequently, AM is being actively explored for the production of zirconia-based restorations<sup>9</sup>.

A critical yet underexplored variable in AM is the printing angle or build orientation. This parameter directly influences layer geometry, interlayer bonding, and manufacturing trajectory, thereby affecting the dimensional, mechanical, and—crucially—the optical properties of the final restoration<sup>8,10,11</sup>. While studies have begun to examine how printing orientation alters mechanical performance<sup>12</sup>, its specific impact on the optical behavior of 3D-printed zirconia—which is fundamental for aesthetic success—remains inadequately investigated, especially in direct comparison to milled counterparts<sup>13,14</sup>.

Given the increasing clinical demand for highly aesthetic, metal-free restorations and the potential of AM to address the limitations of SM, a detailed understanding of the optical characteristics of printed zirconia is essential. This gap in knowledge limits the informed adoption of AM for definitive aesthetic restoration in post-trauma reconstruction. Therefore, the purpose of this *in vitro* study was to evaluate key aesthetic parameters—optical behavior (translucency and gloss)—of dental zirconia fabricated for trauma-related restorations, directly comparing the conventional milling technique with 3D printing across three different printing angles.

## Methods

### Study Design and Setting

This *in vitro* study aimed to evaluate the optical properties of zirconia fabricated using methods relevant to the rapid production of aesthetic dental prostheses in post-trauma reconstruction. Zirconia samples were produced by conventional milling (control) and by digital light processing (DLP) 3D printing at three

different build orientations (0°, 45°, and 90°). To simulate clinical aging, all samples underwent thermocycling equivalent to approximately one year of oral service. The study was conducted at the Department of Dental Prostheses, Faculty of Dentistry, Baqiyatallah University of Medical Sciences, during the 2024–2025 academic year. Ethical approval was obtained from the institutional Ethics Committee (IR.BMSU.BLC.1403.038).

### Sample Preparation

Eighty tetragonal HT zirconia (low Al<sub>2</sub>O<sub>3</sub> content) samples were fabricated using four different methods (20 samples per group) as follows: 15 unglazed square blocks measuring 15 × 15 × 1 mm for translucency evaluation, and 5 unglazed rectangular blocks measuring 7 × 2 cm × 1 mm thick for gloss measurement using a gloss meter (12). A preliminary STL (Standard Tessellation Language) file was created using Meshmixer software (Autodesk Inc., California, USA). This computer-generated CAD file is a standard file that can be used for either milling or 3D printing.

Based on the fabrication method, the samples were divided into four groups (Figure 1):

Group 1 (Control): Milled zirconia (20 samples)

Group 2: Zirconia with 0° print angle (20 samples)

Group 3: Zirconia with 45° print angle (20 samples)

Group 4: Zirconia with 90° print angle (20 samples)

Since milling is the conventional method for producing zirconia in dentistry, this group served as the control, and the three printing groups were compared with it.

### 3D Printing Groups

The samples were prepared using a Zipro printer (AON Co., LTD, Korea) and A0 INNI-CERA zirconia slurry (AON, Korea). The zirconia slurry, with particle sizes ranging from 100 to 900 nm, was processed using vat photopolymerization via digital light processing (DLP). The slurry consisted of zirconia and a UV binder, with a zirconia content exceeding 80%. The UV binder contained a photoinitiator, monomer, oligomer, and additives (16). The printing process was performed under normal atmospheric pressure at a temperature of 25°C and humidity below 70%.

The Inni-Cera slurry contained the following zirconia mixture (mol%): ZrO<sub>2</sub> 92.5, Al<sub>2</sub>O<sub>3</sub> 0.07, SiO<sub>2</sub> 0.58, MgO 0.14, Na<sub>2</sub>O 0.14, K<sub>2</sub>O 0.07, SnO<sub>2</sub> 0.15, Y<sub>2</sub>O<sub>3</sub> 4.6, and HfO<sub>2</sub> [with a percentage between 80–85 wt% before printing and nearly 100% after printing] (17). Printing was performed with a layer thickness of 50 μm according to the manufacturer's recommendation, using three different printing angles: 0°, 45°, and 90° (Figure 2). The pixel size of the printer projector was 40 μm, and the image resolution was 1920 × 1080 pixels.

#### Sintering Process

According to the manufacturer's recommended guidelines, after printing, the samples were subjected to two stages of sintering in an Ivoclar Programat EP 3010 oven (Ivoclar Vivadent AG, Schaan, Liechtenstein, Germany). In the first stage (debinding), the samples were heated in the oven according to the temperature steps shown in table 1 for a total of 11 hours and 30 minutes to clean and remove the binders. Subsequently, in the second stage, the final sintering process was performed for 5 hours according to table 2 (16).

#### Control group (Milling):

The samples were milled from white pre-sintered zirconia blanks (NOVI Dental Product GmbH, IHK, Dusseldorf, Germany) with a Sirona 5-axis milling machine (inlab-MC-X5-Wet-Dry-5-Axis-Miling-and-Grinding-Unit, USA) and a new milling cutter and then sintered in a Programat EP 3010 furnace (Ivoclar Vivadent AG Schaan, Liechtenstein, Germany) at 1500°C for 90 minutes (according to the manufacturer's instructions).

#### Thermocycling:

All samples were subjected to 10,000 thermal cycles in a thermocycler (Dorsa, Iran) to simulate the aging process using cyclic temperature changes equivalent to 1 year (18). The parameters for thermal cycling of the samples were as follows:

- Hot bath temperature: 55°C/131°F
- Cold bath temperature: 5°C/41°F
- Dwell time (hot and cold): 30 seconds
- Drain time: 5 seconds

#### Translucency Parameter:

After sample preparation, translucency measurements were performed based on the CIE L\*a\*b\* color scale relative to the CIE standard illuminant D65, where L\* refers to the degree of brightness (0-100), a\* refers to the color coordinate on the red/green axis, and b\* refers to the color coordinate on the yellow/blue axis. TP was

measured by evaluating the color difference of the samples on a black background (CIE L\* = 7.61, a\* = 0.45, b\* = 2.42) and a white background (CIE L\* = 88.81, a\* = -4.98, b\* = 6.09).

TP ½ calculation formula:  $TP = [(L^*b - L^*w)^2 + (a^*b - a^*w)^2 + (b^*b - b^*w)^2]$

TP - transparency parameter L\* - degree of brightness  
a\* - color coordinate on the red/green axis  
b\* - color coordinate on the yellow/blue axis

The subscripts b and w refer to the color coordinates against a black and white background, respectively.

The CIE Lab color scale was measured using a spectrophotometer (X-rite, USA). The instrument was calibrated before the measurements, and the probe tip was perpendicular to the center of the samples. The color coordinates inside the Viewing Booth were measured using D65 Standard Illuminant (19). The room temperature was between 15 and 40°C as recommended by the manufacturer. The optical parameters to be evaluated were measured 3 consecutive times before and after the thermal cycle and the average values were recorded.

#### Gloss:

The gloss of the samples was measured using a micro-TRI-gloss ASTM D523 Gloss Meter (BYK Gardner-Germany) located at the Institute of Color Science and Technology. The glossmeter has an 85° light source, 7 cm × 2 cm optical aperture dimensions, and a 0–100 Gu capability. Gloss measurements were taken from the center of each sample and five times for each area before and after thermal cycling, and the average values were reported for each sample. All measurements were performed in a controlled light environment to help limit incidental light contamination. The device measured the light reflectance of a surface by shining light at an 85° angle onto the surface and measuring the reflected light (20).

#### Data analysis method:

Considering the normality of the data distribution based on the Shapiro-Wilk test and the skewness and kurtosis indices, one-way analysis of variance (ANOVA) was used to compare the changes between different groups. Tukey Post Hoc Test was also used for paired comparisons. Paired Sample T-Test was used for intra-group comparisons before and after the time. All statistical analyses were performed using SPSS version 24 software and the statistical significance level was set at 5%.

Table 1. Debinding protocol for print samples

Step	Start Temp (°C)	End Temp (°C)	Rising Temp (°C)	Ramp-up Rate (°C/min)	Time (Min)	Total Time
1	0	150	150	10	15	11h 31m Single veneer, Coping, bracket
2	150	200	50	5	10	
3	200	320	120	0.3	400 (6h 40m)	
4	320	320	0	0	30 (hold)	
5	320	490	170	2	85 (1h 25m)	
6	490	490	0	0	30 (hold)	
7	490	1100	610	10	61	
8	1100	1100	0	0	60 (hold)	

Table 2: Final sintering protocol for printed samples

Step	Start Temp (°C)	End Temp (°C)	Rising Temp (°C)	Ramp-up Rate (°C/min)	Time (Min)	Total Time
1	0	1200	1200	10	120 (2h)	5h
2	1200	1500	300	5	60 (1h)	Sintering post-debinding & coloring
3	1500	1500	0	0	120 (2h hold)	

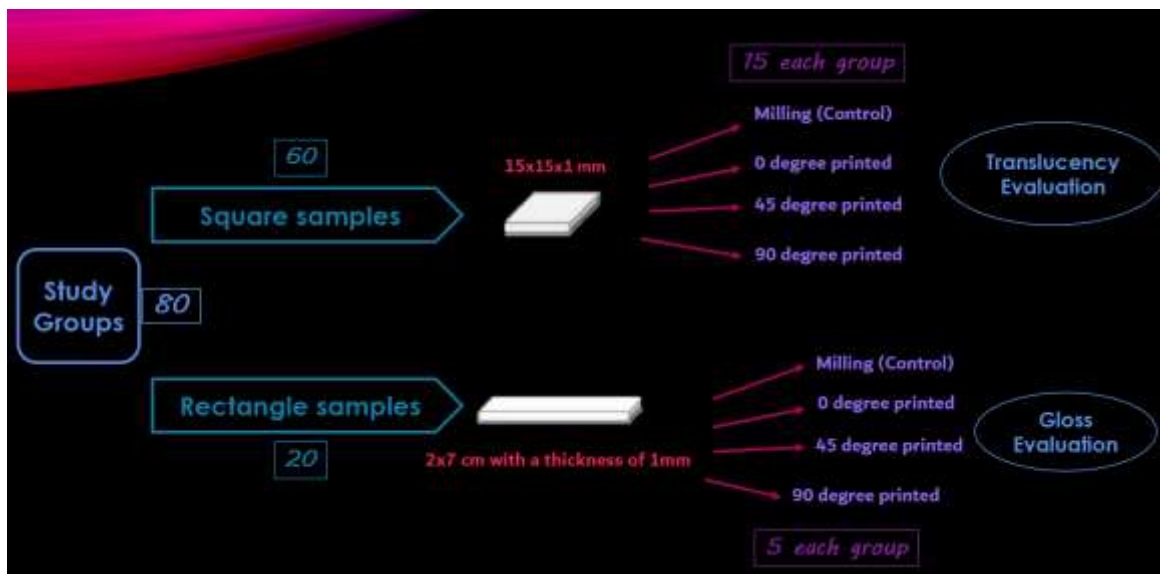


Figure 1: Schematic image of study groups.

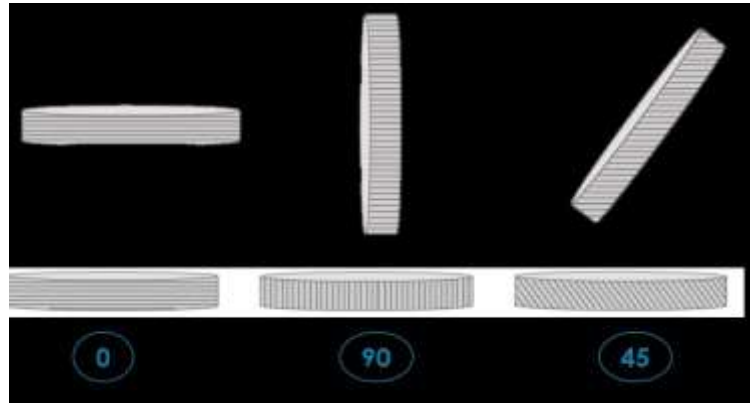


Figure 2: Schematic view of the printing angles used in the study



Figure 3: Zirconia samples fabricated for Translucency evaluation



Figure 4: Zirconia samples fabricated for surface Gloss evaluation

## Results

The result show that the TP and GLOSS variables in all study groups before and after thermocycling had skewness in the range of -2 to +2, and the Shapiro-Wilk test also showed that they had a normal distribution ( $p < 0.05$ ).

### Examination of the TP variable

In this study, before thermocycling, the lowest TP value was related to 90 degrees and the highest value was related to Milling, while after thermocycling, the lowest value was related to 45 degrees, and the highest value was related to Milling.

Although we encountered a decrease in TP value in the Milling and 45-degree groups, this decrease was not statistically significant. ( $P < 0.05$ ). However, in the two

0- and 90-degree groups, although the TP value increased slightly after thermocycling, this increase was also not statistically significant ( $P < 0.05$ ) (Table 3). In other words, intra-group comparisons showed that thermocycling had no effect on the TP variable. Also, comparing the amount of changes using the analysis of variance test showed that there was no significant difference between the study groups ( $P = 0.145$ ). In other words, the manufacturing method had no effect on TP value.

#### Examination of the GLOSS variable

In this study, both before and after thermocycling, the value of Gloss in the Milling group had the highest value and the 90-degree group had the lowest value.

The results of this study showed that there was a significant difference in all study groups from before to after thermocycling ( $P < 0.001$ ) (Table 4). In other words, the thermocycling performed was effective in all groups. Also, the analysis of changes before and after thermocycling by analysis of variance test showed that there was a significant difference between the study groups ( $P = 0.019$ ). Tukey's post hoc test showed that the 0 degree and milling groups ( $P = 0.043$ ), 0 degree and 45 degree ( $P = 0.024$ ), and 0 degree and 90 degree ( $P = 0.046$ ) had a significant difference, but no significant difference was seen in comparison with the other groups ( $P < 0.05$ ) (Table 5).

Table 3: Translucency Parameter (TP) Values Before and After Thermocycling

Study Group	Pre-Thermocycling <i>M (SD)</i>	Post-Thermocycling <i>M (SD)</i>	Difference (Post - Pre) <i>M (SD)</i>	* <i>p</i> *-value (Paired * <i>t</i> *-test)
<b>Milled (Control)</b>	8.08 (0.44)	7.84 (0.48)	-0.27 (1.04)	.238
<b>0° Printed</b>	7.37 (0.53)	7.59 (0.84)	0.22 (1.06)	.475
<b>45° Printed</b>	7.17 (0.53)	7.10 (0.89)	-0.07 (1.12)	.363
<b>90° Printed</b>	7.45 (0.72)	7.01 (1.06)	-0.44 (1.55)	.038

Note. M = Mean, SD = Standard Deviation; n = 15 per group for TP measurement.

Table 4: Surface Gloss (GU) Values Before and After Thermocycling

Study Group	Pre-Thermocycling <i>M (SD)</i>	Post-Thermocycling <i>M (SD)</i>	Difference (Post - Pre) <i>M (SD)</i>	* <i>p</i> *-value (Paired * <i>t</i> *-test)
<b>Milled (Control)</b>	79.42 (0.64)	77.31 (0.68)	-2.11 (0.27)	< .001
<b>0° Printed</b>	73.20 (0.53)	71.45 (0.56)	-1.75 (0.19)	< .001
<b>45° Printed</b>	68.48 (0.48)	66.32 (0.58)	-2.16 (0.11)	< .001
<b>90° Printed</b>	62.21 (0.36)	60.11 (0.28)	-2.10 (0.20)	< .001

Note. M = Mean, SD = Standard Deviation; n = 5 per group for gloss measurement.

Table 5: Post-Hoc Pairwise Comparisons (Tukey HSD) for Change in Gloss ( $\Delta$ Gloss)

Comparison	Mean Difference	* <i>p</i> *-value	
Group 1	Group 2		
<b>Milled (Control)</b>	0° Printed	-0.36	.043
	45° Printed	0.05	.974
	90° Printed	-0.01	.999
<b>0° Printed</b>	45° Printed	0.41	.024
	90° Printed	0.35	.046
<b>45° Printed</b>	90° Printed	-0.06	.954

## Discussion

The optical integration of dental restorations is a critical component in the rehabilitation of craniomaxillofacial (CMF) trauma, where restoring aesthetics is fundamental to a patient's psychosocial

recovery. This in vitro study evaluated key optical properties—translucency and gloss—of zirconia fabricated via conventional milling and via 3D printing at various angles, simulating clinical aging. The principal finding is that while translucency remained stable across fabrication methods and

after aging, surface gloss was significantly influenced by both the manufacturing technique and thermocycling. This distinction has direct implications for selecting fabrication strategies in time-sensitive trauma care.

Color science provides an objective framework for evaluating the optical performance of dental materials, particularly in terms of translucency and surface appearance. In the present study, the optical behavior of dental zirconia fabricated by milling and additive manufacturing at different printing angles was investigated by assessing translucency and gloss before and after thermocycling. The results demonstrated that neither the fabrication method nor thermocycling significantly affected the translucency parameter (TP), whereas surface gloss was strongly influenced by both the manufacturing approach and the applied aging protocol.

Translucency is a key optical parameter for achieving a natural tooth-like appearance and is influenced by several microstructural characteristics of zirconia, including grain size, phase composition, porosity, and sintering conditions<sup>22,23</sup>. In particular, the presence of optically isotropic cubic phases has been shown to reduce light scattering caused by birefringence, thereby enhancing translucency<sup>24,25</sup>. In the present study, the absence of significant differences in TP values among the milled and 3D-printed groups suggests that the overall microstructural features governing light transmission were not substantially altered by the fabrication method or printing orientation under the applied processing conditions. The findings of the present study are consistent with previous reports indicating that artificial aging procedures, such as thermocycling, may have a limited effect on the translucency of high-translucency zirconia materials. de Araújo-Júnior et al. reported no significant changes in the translucency of 5Y-PSZ zirconia following aging protocols, which aligns with the results observed in this study<sup>30</sup>. Similar outcomes have also been

reported for different zirconia generations subjected to thermocycling or hydrothermal aging<sup>31-33</sup>. Variations among published results can be attributed to differences in material composition, yttria content, sintering parameters, specimen thickness, and measurement conditions, which limit direct numerical comparisons between studies.

In contrast to translucency, surface gloss was significantly affected by both the fabrication method and thermocycling. The results of the present study demonstrated a consistent reduction in gloss values following thermocycling across all groups, indicating that artificial aging plays a critical role in altering the surface-related optical characteristics of zirconia. Additionally, the fabrication method significantly influenced gloss values, with milled zirconia specimens exhibiting the highest gloss and samples printed at a 90° orientation showing the lowest values both before and after thermocycling.

The observed decrease in surface gloss after thermocycling can be explained by changes occurring at the material surface during repeated thermal stress and water exposure. Thermocycling may promote microstructural alterations, such as increased surface roughness or microcrack formation, which enhance light scattering and reduce specular reflection. Since gloss is highly sensitive to surface topography, even subtle surface irregularities induced by aging can lead to a measurable decline in gloss values.

Limited studies have specifically evaluated the gloss of zirconia using standardized gloss measurement devices. However, previous investigations comparing additively manufactured and milled zirconia have reported higher surface roughness in 3D-printed specimens, which indirectly supports the findings of the present study<sup>34</sup>.

Increased surface roughness is known to reduce gloss by disrupting regular light reflection, thereby providing a plausible explanation for the lower gloss values observed in printed samples compared

to milled zirconia.

Among the additively manufactured groups, printing orientation played a decisive role in determining surface gloss. Specimens printed at a 0° orientation exhibited significantly higher gloss values compared to those printed at 45° and 90°, both before and after thermocycling. This finding can be attributed to the layer-by-layer deposition pattern inherent to additive manufacturing, where printing orientation influences layer alignment and surface continuity. At lower printing angles, the outer surface appears more uniform, whereas steeper angles result in pronounced staircase-like surface features that increase surface irregularities and reduce gloss.

From a clinical and manufacturing perspective, these findings highlight the importance of optimizing printing orientation when fabricating zirconia restorations using additive manufacturing techniques. While translucency appears to be relatively insensitive to printing angles, surface gloss—which contributes significantly to the perceived aesthetic quality of restorations—is strongly affected by build orientation. Therefore, selecting appropriate printing angles may reduce the need for extensive post-processing procedures and improve the overall aesthetic outcome of 3D-printed zirconia restorations.

## Conclusion

In this *in vitro* investigation, we found that while fabrication method and artificial aging did not significantly affect the translucency of dental zirconia, surface gloss was substantially influenced by both manufacturing approach and printing orientation. Milled zirconia demonstrated higher gloss values compared to specimens produced by additive manufacturing. Furthermore, among the printed groups, lower printing angles were associated with enhanced surface sheen. Thermocycling consistently reduced gloss across all conditions, underscoring the importance of surface characteristics for long-term aesthetic

performance. These findings contribute to a deeper understanding of how digital fabrication parameters influence the key optical properties of zirconia restorations and may guide clinicians and technicians in optimizing manufacturing strategies to achieve desirable aesthetic outcomes.

## Acknowledgments

None.

## Conflict of Interest Disclosures

The authors have no relevant financial or non-financial interests to disclose.

## Funding Sources

None.

## Authors' Contributions

Conceptualization, E.M. and N.N.; methodology, E.M. and E.T.; investigation, E.M.; data curation, E.M. and E.T.; writing—original draft preparation, E.M.; writing—review and editing, N.N. and E.T.; supervision, N.N. All authors have read and agreed to the published version of the manuscript.

## Ethical Statement

This study was registered with the ethical code (IR.BMSU.BLC.1403.076) and in the history of Baqiyatullah University of Medical Sciences.

## Declaration of Generative AI and AI-assisted technologies

Not cleared.

## References

1. Su G, Zhang Y, Jin C, Zhang Q, Lu J, Liu Z, et al. 3D printed zirconia used as dental materials: a critical review. *J Biol Eng* 2023;17(1):78.
2. Camargo B, Willems E, Jacobs W, Van Landuyt K, Peumans M, Zhang F, et al. 3D printing and milling accuracy influence full-contour zirconia crown adaptation. *Dent Mater* 2022;38(12):1963-76.
3. Lerner H, Nagy K, Pranno N, Zarone F, Admakin O, Mangano F. Trueness and precision of 3D-printed versus milled monolithic zirconia crowns: An *in vitro* study. *J Dent* 2021;113:103792.
4. Rexhepi I, Santilli M, D'Addazio G, Tafuri G, Manciocchi E, Caputi S, et al. Clinical applications and mechanical properties of cad-cam materials in restorative and prosthetic

- dentistry: A systematic review. *J Funct Biomater* 2023;14(8):431.
5. Dewan H. Clinical Effectiveness of 3D-Milled and 3D-Printed Zirconia Prosthesis—A Systematic Review and Meta-Analysis. *Biomimetics* 2023;8(5):394.
  6. Buj-Corral I, Vidal D, Tejo-Otero A, Padilla JA, Xuriguera E, Fenollosa-Artés F. Characterization of 3D printed yttria-stabilized zirconia parts for use in prostheses. *Nanomaterials* 2021;11(11):2942.
  7. Bergler M, Korostoff J, Torrecillas-Martinez L, Mante FK. Ceramic Printing--Comparative Study of the Flexural Strength of 3D-Printed and Milled Zirconia. *Int J Prosthodont* 2022;35(6):777–83.
  8. Branco AC, Colazo R, Figueiredo-Pina CG, Serro AP. Recent advances on 3D-printed zirconia-based dental materials: a review. *Materials* 2023;16(5):1860.
  9. Methani MM, Revilla-León M, Zandinejad A. The potential of additive manufacturing technologies and their processing parameters for the fabrication of all-ceramic crowns: A review. *Esthet Restor Dent* 2020;32(2):182-92.
  10. Espinar C, Della Bona A, Páez MM, Tejada-Casado M, Pulgar R. The influence of printing angle on color and translucency of 3D printed resins for dental restorations. *Dent Mater* 2023;39(4):410-7.
  11. Espinar C, Della Bona A, Tejada-Casado M, Pulgar R, Páez MM. Optical behavior of 3D-printed dental restorative resins: Influence of thickness and printing angle. *Dent Mater* 2023;39(10):894-902.
  12. Xiang D, Xu Y, Bai W, Lin H. Dental zirconia fabricated by stereolithography: Accuracy, translucency and mechanical properties in different build orientations. *Ceram Int* 2021;47(20):28837-47.
  13. Espinar C, Della Bona A, Páez MM, Pulgar R. Color and optical properties of 3D printing restorative polymer-based materials: A scoping review. *J Esthet Restor Dent* 2022;34(6):853-64.
  14. Schweiger J, Edelhoff D, Geth JF. 3D printing in digital prosthetic dentistry: an overview of recent developments in additive manufacturing. *J Clin Med* 2021;10(9):2010.
  15. Marsico C, Šilo M, Kutsch J, Kauf M, Arola D. Vat polymerization-printed partially stabilized zirconia: Mechanical properties, reliability and structural defects. *Addit Manuf* 2020;36:101450.
  16. Kim SH, Oh NS, Pang NS, Jung BY. The effect of surface treatment and low-temperature degradation on flexural strength of additive manufactured zirconia. *J Mech Behav Biomed Mater* 2023;148:106167.
  17. Polychronis G, Papageorgiou SN, Riollo CS, Panayi N, Zinelis S, Eliades T. Fracture toughness and hardness of in-office, 3D-printed ceramic brackets. *Orthod Craniofac Res* 2023;26(3):476-80.
  18. Taşın S, Ismatullaev A. Comparative evaluation of the effect of thermocycling on the mechanical properties of conventionally polymerized, CAD-CAM milled, and 3D-printed interim materials. *J Prosthet Dent* 2022;127(1):173-e1.
  19. Kilinc H, Turgut S. Optical behaviors of esthetic CAD-CAM restorations after different surface finishing and polishing procedures and UV aging: An in vitro study. *J Prosthet Dent* 2018;120(1):107-13.
  20. Vance M, Lawson NC, Rupal M, Beck P, Burgess JO. Color and gloss of nano-filled resin-modified glass ionomers and resin composites. *Esthet Restor Dent* 2015;27(5):293-9.
  21. Salama AA, Shehab KA, Bushra SS, Hamza FS. The effect of aging on the translucency of contemporary zirconia generations: in-vitro study. *BMC Oral Health* 2024;24(1):744.
  22. Jerman E, Lymkemann N, Eichberger M, Zoller C, Nothelfer S, Kienle A, et al. Evaluation of translucency, Marten's hardness, biaxial flexural strength and fracture toughness of 3Y-TZP, 4Y-TZP and 5Y-TZP materials. *Dent Mater* 2021;37(2):212-22.
  23. Cinar S, Altan B. Effect of Veneering and Hydrothermal Aging on the Translucency of Newly Introduced Extra Translucent and High Translucent Zirconia with Different Thicknesses. *Biomed Res Int* 2021;2021:7011021.
  24. Klimke J, Trunec M, Krell A. Transparent tetragonal yttria-stabilized zirconia ceramics: influence of scattering caused by birefringence. *J Am Ceram Soc* 2011;94(6):1850-8.
  25. Zhang Y. Making yttria-stabilized tetragonal zirconia translucent. *Dent Mater* 2014;30(10):1195-203.
  26. Kontonasaki E, Rigos AE, Ilia C, Istantos T. Monolithic Zirconia: An Update to Current Knowledge. Optical Properties, Wear, and Clinical Performance. *Dent J (Basel)* 2019;7.(3)
  27. Yamashita I, Tsukuma K. Light scattering by residual pores in transparent zirconia ceramics. *J Ceram Soc Jpn* 2011;119(1386):133-5.
  28. Yu B, Ahn JS, Lee YK. Measurement of translucency of tooth enamel and dentin. *Acta Odontol Scand* 2009;67(1):57-64.
  29. Pop-Ciutrla IS, Ghinea R, Colosi HA, Dudea D. Dentin translucency and color evaluation in human incisors, canines, and molars. *J Prosthet Dent* 2016;115(4):475-81.
  30. de Araújo-Junior ENS, Bergamo ETP, Bastos TMC, Benalcázar Jalkh EB, Lopes ACO, Monteiro KN, et al. Ultra-translucent zirconia processing and aging effect on microstructural, optical, and mechanical properties. *Dent Mater* 2022;38(4):587-600.
  31. Hajhamid B, Bozec L, Tenenbaum H, De Souza G, Somogyi-Ganss E. Effect of artificial aging on optical properties and crystalline structure of high-translucency zirconia. *J Prosthodont* 2024;33(1):61-9.
  32. Alraheam IA, Donovan TE, Rodgers B, Boushell L, Sulaiman TA. Effect of masticatory simulation on the translucency of different types of dental zirconia. *J Prosthet Dent* 2019;122(4):404-9.
  33. Lymkemann N, Stawarczyk B. Impact of hydrothermal aging on the light transmittance and flexural strength of colored yttria-stabilized zirconia materials of different formulations. *J Prosthet Dent* 2021;125(3):518-26.
  34. Hassan RM, Ibrahim Y, Abo ERG, Azer AS. Evaluation of fracture resistance and surface characteristics in monolithic zirconia: a comparative analysis of 3D printing and milling techniques. *BMC Oral Health* 2025;25(1):1236.
  35. Shin JW, Kim JE, Choi YJ, Shin SH, Nam NE, Shim JS, et al. Evaluation of the Color Stability of 3D-Printed Crown and

Bridge Materials against Various Sources of Discoloration: An In Vitro Study. *Materials (Basel)* 2020;13-(23)

36. Song SY, Shin YH, Lee JY, Shin SW. Color stability of provisional restorative materials with different fabrication methods. *J Adv Prosthodont* 2020;12(5):259-64.
37. Jain S, Sayed ME, Shetty M, Alqahtani SM, Al Wadei MHD, Gupta SG, et al. Physical and Mechanical Properties of 3D-Printed Provisional Crowns and Fixed Dental Prosthesis Resins Compared to CAD/CAM Milled and Conventional Provisional Resins: A Systematic Review and Meta-Analysis. *Polymers (Basel)* 2022;14.(13)
38. Bradfield J. The perception of gloss: a comparison of three methods for studying intentionally polished bone tools. *J Archaeol Sci* 2020;32:102425.